

Inducing spin-correlations and entanglement in a double quantum dot through non-equilibrium transport

C. A. Büsser¹ and F. Heidrich-Meisner^{1,2}

¹Department of Physics and Arnold Sommerfeld Center for Theoretical Physics, Ludwig-Maximilians-University Munich, Germany*

²Institute for Theoretical Physics II, Friedrich-Alexander University Erlangen-Nuremberg, Germany

For a double quantum dot system in a parallel geometry, we demonstrate that by combining the effects of a flux and driving an electrical current through the structure, the spin correlations between electrons localized in the dots can be controlled at will. In particular, a current can induce spin correlations even if the spins are uncorrelated in the initial equilibrium state. Therefore, we are able to engineer an entangled state in this double-dot structure. We take many-body correlations fully into account by simulating the real-time dynamics using the time-dependent density matrix renormalization group method. Using a canonical transformation, we provide an intuitive explanation for our results, related to Ruderman-Kittel-Kasuya-Yoshida physics driven by the bias.

PACS numbers: 73.23.Hk, 72.15.Qm, 73.63.Kv

Introduction: Considerable progress in nanotechnology in the last decades has made possible the fabrication of new artificial structures [1] such as quantum dots (QDs), quantum rings, or molecular conductors. The physics of quantum dots in a parallel geometry is intriguing, since it allows one to study interference effects between electrons traveling through different paths, most notably realized in the Aharonov-Bohm effect. Such structures have been studied in several experiments [2, 3]. Besides the interest in practical applications in nanoelectronics or in fundamental many-body physics such as the Kondo effect [3], double quantum dots (DQD) also play a vital role in the context of quantum information processing [4–6]. Generating, controlling, and detecting entangled states in condensed matter systems is one of the challenges for future quantum computation applications [7]. Various proposals for entangling spatially separated electrons have been put forward, such as, for instance, by splitting Cooper pairs [8, 9] or by manipulating spins in quantum dots [10]. In a DQD, an entangled state can be realized by putting the electrons into a singlet state [4, 5, 11]. Means of detecting entangled states of electrons were discussed in, e.g., Refs. [8, 12].

In this work, we demonstrate that an entangled state between electrons localized in a DQD embedded in an Aharonov-Bohm interferometer can be induced and controlled by sending an electrical current through the structure. In the presence of a flux, the initial state can even be fully uncorrelated yet the non-equilibrium dynamics results in non-zero spin correlations in the steady state. The sign and the strength of such steady-state spin correlations depend on voltage, interactions, and the flux. The generation of entanglement through non-equilibrium dynamics in quantum dots, with different set-ups, has been discussed in Refs. [13]. An additional motivation for our work stems from the current interest, both from theory [14, 15] and from experiment (see, e.g., [16]), in the real-time and non-equilibrium dynamics of nano-structures with strong electronic correlations. An important aspect is that we can treat both interactions and non-equilibrium dynamics in a well-controlled manner using the time-dependent density matrix renormalization

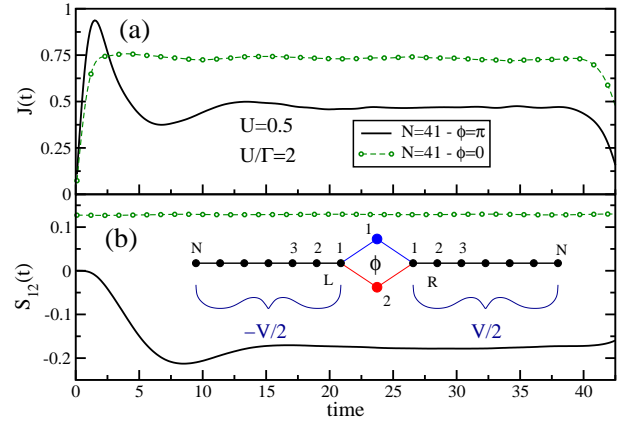


FIG. 1. (Color online) Current and spin correlations as a function of time. (a) Current $J(t)$ for $\phi = 0$ and π , $V = 0.50$. (b) Spin correlation $S_{12}(t)$. All for $N = 41$, $U = 0.5$, $V = 0.5$. Inset in (b): Sketch of the DQD structure studied here.

group (DMRG) method [17].

The model: We study a system of two quantum dots in a parallel geometry represented by two Anderson impurities, as sketched in Fig. 1(b). The Hamiltonian is

$$H = H_1 + H_{hy1} + H_{hy2} + H_{int}, \quad (1)$$

$$H_1 = \sum_{\alpha=L,R} \sum_{i=1; \sigma}^{N-1} \left[-t_0 (c_{\alpha i \sigma}^\dagger c_{\alpha i+1 \sigma} + h.c.) \right] + \sum_{\alpha=L,R} \sum_{i=1; \sigma}^N \mu_\alpha n_{\alpha i \sigma}, \quad (2)$$

$$H_{hy1} = -t'_1 [d_{1\sigma}^\dagger c_{L1\sigma} + c_{R1\sigma}^\dagger d_{1\sigma} + h.c.], \quad (3)$$

$$H_{hy2} = -t'_2 [d_{2\sigma}^\dagger c_{L1\sigma} + e^{i\phi} c_{R1\sigma}^\dagger d_{2\sigma} + h.c.], \quad (4)$$

$$H_{int} = \sum_{j=1,2; \sigma} [U n_{j\sigma} n_{j\bar{\sigma}} + V_g n_{j\sigma}]. \quad (5)$$

The system size is $2N + 2$ where N is the number of sites in the left or right lead. The two dots are at the center of the system labeled by $j = 1, 2$. The Hamiltonian consists of

four parts: First, the non-interacting leads H_1 with a constant hopping matrix element $t_0 = 1$ used as the unit of energy ($\hbar = 1, e = 1$). Second, the terms H_{hy1} and H_{hy2} give rise to the hybridization between the localized levels of the dots and the leads. If not stated otherwise, we consider fully symmetric tunnel couplings, i.e., $t'_1 = t'_2 = t'$ (see the supplementary material [18] for a discussion of asymmetric couplings). We define the tunneling strength by $\Gamma = 2\pi t'^2 \rho_{\text{leads}}(E_F) = 2t'^2$, where $\rho_{\text{leads}}(E_F)$ is the local density of states (LDOS) of the leads at the Fermi energy E_F . In the hopping matrix element between the second dot and the right lead we incorporate an arbitrary phase ϕ that will be important in our study. Finally, there is the interacting region H_{int} with the two quantum dots, which are both subject to the same Coulomb repulsion U and a gate potential $V_g = -U/2$ such that both dots are kept at half filling. The operator $c_{\alpha l \sigma}^\dagger$ ($c_{\alpha l \sigma}$) creates (annihilates) an electron at site l in the $\alpha = L, R$ lead with spin σ while $d_{j\sigma}^\dagger$ ($d_{j\sigma}$) acts on dot j ; $n_{\alpha l \sigma} = c_{\alpha l \sigma}^\dagger c_{\alpha l \sigma}$ as usual. In Eq. (2), μ_L and μ_R mimic the chemical potentials of the leads.

The ground state and the linear conductance of DQDs Eq. (1) were extensively studied in Ref. [19]. A closely related DQD model with a finite flux ϕ and with spin-polarized electrons was discussed in Ref. [20].

The phase included in Eq. (4) may have a different meaning depending on the specific physical realization. The most obvious one is to associate ϕ with a magnetic flux that pierces the ring structure containing the two dots and the first site from each lead as shown in Fig. 1(b). As usual, one can use a gauge transformation such that the flux appears in only one of the four hopping matrix elements.

Another situation that can be described by this Hamiltonian is a single quantum dot with two levels. Depending on the filling of a QD, two degenerate levels may exist that can couple differently to the leads. As an example of this latter case let us consider a spherical QD weakly coupled to the leads. The angular part of the QD's eigenfunctions are spherical harmonics Y_{lm} . Let us suppose that the weak contact with the leads are along the z -axis, and discuss the coupling of p_μ -orbitals ($\mu = x, y, z$). The p_z orbitals have an opposite weight for opposite z -coordinates creating a phase difference of $\phi = \pi$ in the hopping terms to the leads. The other two orbitals p_x and p_y lack this extra phase by symmetry. This example illustrates that different phases for different orbitals of a single QD are possible once they are coupled to the leads through the hybridization. Note that in the first example, ϕ can take arbitrary values $\phi \in [0, \pi]$, whereas in the second case, only $\phi = 0, \pi$ are possible.

We use DMRG [17] to obtain the steady state in the presence of a finite bias voltage by time-evolving the wavefunction $|\Psi(t)\rangle$ and then its properties such as the current and spin correlations as a function of time t . This method has been successfully used to study non-equilibrium transport through nano-structures with electronic correlations [14, 21, 22]. We measure the spin correlations by evaluating [23]

$$S_{12}(t) = \langle \Psi(t) | \vec{S}_1 \cdot \vec{S}_2 | \Psi(t) \rangle. \quad (6)$$

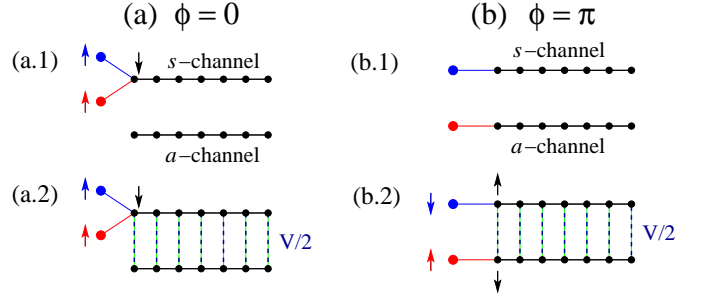


FIG. 2. (Color online) *Illustration of the canonical transformation used to understand the non-equilibrium spin correlations.* (a) $\phi = 0$. (b) $\phi = \pi$. The upper two panels (a.1) and (b.1) show the situation for $V = 0$, whereas (a.2) and (b.2) are for $V \neq 0$. The application of the bias leads to a ladder structure where the bias acts like a transverse hopping matrix element between the symmetric (s -channel) and antisymmetric states (a -channel) defined in Eq. (8).

The current between two sites in the leads is defined as

$$J_{l,m}(t) = it_0 \sum_{\sigma} \langle \Psi(t) | c_{l\sigma}^\dagger c_{m\sigma} - c_{m\sigma}^\dagger c_{l\sigma} | \Psi(t) \rangle. \quad (7)$$

In the figures, we display the current $J = (J_{L2,L1} + J_{R1,R2})/2$ averaged over the first link in the left and right lead.

Our simulations start from the system in equilibrium with a finite $\Gamma \neq 0$ and a charge per spin of $\langle n_{j\sigma} \rangle = 0.5$ on both dots. At time $t = 0$, we turn on a bias voltage $V = \mu_L - \mu_R$ that drives the system out of equilibrium. We work at large values of $\Gamma = 0.25$ such that the transient dynamics to reach the steady state is short [22]. During the time-evolution, we use time steps of $\delta t \sim 0.1$ and enforce a fixed discarded weight [24] of 10^{-5} or less, keeping a maximum of 2000 DMRG states. All runs are performed at an overall half filling of dots and leads.

Results: In Fig. 1, we elucidate the time-dependence of the current and spin correlations, comparing the behavior of $\phi = 0$ to $\phi = \pi$. Similar to a single quantum dot [22], the current undergoes transient dynamics, and then takes a quasi-stationary value (i.e., a plateau in time), which we shall refer to as the steady-state regime. Since we work with leads of a finite length, ultimately, the steady-state current decays and changes its sign [22]. The comparison with other methods shows that DMRG correctly captures properties of the true steady state as system size increases [14].

For the spin correlations shown in Fig. 1(b), we first observe that in the initial state, $S_{12} > 0$ for $\phi = 0$ whereas the correlation vanishes for $\phi = \pi$. The application of the bias voltage does virtually not affect the value of S_{12} for $\phi = 0$, which remains positive in our simulations. The more interesting behavior is realized for $\phi = \pi$. As a function of time, S_{12} decreases and approaches a roughly constant value. The transient time seems to be comparable to the one for the current and is of order $1/\Gamma$. Moreover, the transients are suppressed by increasing the bias, similar to a single quantum dot [22]. This finite and large spin correlation between the spins local-

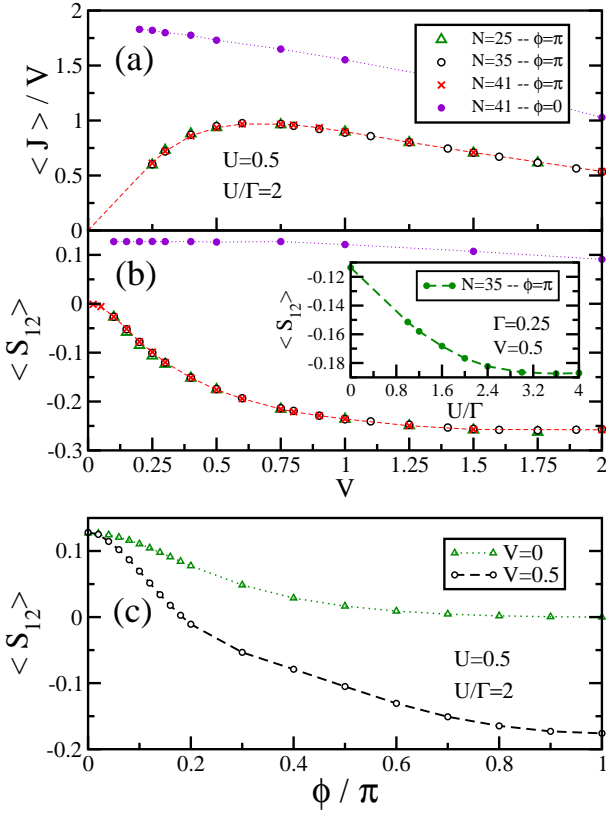


FIG. 3. (Color online) Current and spin correlations as a function of bias V and phase ϕ . (a) $\langle J \rangle / V$ vs. V for $\phi = 0$ and $\phi = \pi$ in units of twice the conductance quantum G_0 . (b) Steady-state spin correlations $\langle S_{12} \rangle$ vs. bias V . The figure shows data for different system sizes $N = 25, 35, 41$ for $\phi = \pi$, with very little finite-size dependencies. In (a) and (b), $U/\Gamma = 2$. Inset in (b): Steady-state spin correlations vs. U/Γ for $V = 0.5$. (c) Spin correlations $\langle S_{12} \rangle$ vs. ϕ for $V = 0$ and in the steady state with $V = 0.5$.

ized in the dots that emerges in the steady state and that is induced by driving a current through the structure is the main aspect of our work. It implies that non-equilibrium dynamics can be used to prepare a DQD in a correlated and thus entangled state.

The qualitative behavior of the spin correlations can be understood by using a canonical transformation of the states of the leads, which is given by (see, e.g., [20, 25]):

$$c_{\gamma l \sigma} = (c_{Rl\sigma} \pm c_{Ll\sigma})/\sqrt{2}, \quad (8)$$

where $\gamma = s, a$ are the symmetric and antisymmetric combinations, respectively. The result of this transformation is sketched in Fig. 2, where the leads shown there now represent the new states obtained from Eq. (8). In the absence of a bias voltage, there is no direct coupling between these new states, as depicted in Figs. 2(a.1) and (b.1). Most importantly, the dots are coupled to only the symmetric states for $\phi = 0$, whereas for $\phi = \pi$, dot $j = 1$ is coupled to the symmetric states and dot $j = 2$ to the antisymmetric ones. For $\phi = 0$, the Ruderman-Kittel-Kasuya-Yoshida (RKKY) interaction gives

rise to a ferromagnetic correlation between the dots since each path that connects them involves an odd number of sites and since the leads are at half-filling [19]. For $\phi = \pi$, the dots are part of two decoupled subsystems and therefore, S_{12} vanishes.

Upon applying a bias, one effectively obtains a ladder geometry where the voltage acts as a transverse coupling between the symmetric and antisymmetric states of Eq. (8) as shown in Figs. 2(a.2) and (b.2). For $\phi = 0$, the coupling V only marginally affects the correlations. By contrast, for $\phi = \pi$ and $V \neq 0$, the dots are now connected through paths with an even number of sites in the effective leads and therefore, in the *ground state* of such a geometry, one expects a finite negative spin correlation. Our numerical results shown in Fig. 1(b) unveil that the same behavior occurs in *non-equilibrium* as well. While here we focus on fully symmetric tunnel couplings, the main results can be recovered in the case of asymmetric couplings [18], and therefore, fine-tuning of parameters is not necessary to observe a change of S_{12} induced by a bias V .

After qualitatively explaining the emergence of finite spin-correlations in the current-carrying stationary state, we next study the dependence of the steady-state properties on the bias potential. We denote the steady-state values by $\langle S_{12} \rangle$ and $\langle J \rangle$, obtained from averaging over time-dependent data in the steady-state regime (compare Ref. [22]). Figure 3(a) shows $\langle J \rangle / V$ versus V for phases $\phi = 0$ and π . For $\phi = 0$, $\langle J \rangle / V$ approaches a constant value at low bias [19] (an extended analysis of the current-voltage characteristics of our DQD structure will be presented elsewhere). For $\phi = \pi$, the linear conductance vanishes due to the Aharonov-Bohm effect [20]. A finite voltage causes a finite current to flow in both cases, but $\langle J \rangle / V$ for $\phi = 0$ is always larger than in the $\phi = \pi$ case.

In Fig. 3(b), we show the steady-state spin correlations $\langle S_{12} \rangle$ versus V . First, let us emphasize that data for the steady-state values obtained from systems of different lengths are included, showing that all our main results are quantitatively robust against finite-size effects. For $\phi = 0$, a constant value of $\langle S_{12} \rangle > 0$ is found. A slight decrease appears for $V \gtrsim 1$, which we trace back to the variation of the LDOS of the leads seen by the dots. Since in our simulations we work with tight-binding bands with a finite band-width and band curvature, this LDOS decreases with V . For the case of $\phi = \pi$, the value of the steady-state correlations can be tuned by the bias voltage. As the figure clearly shows, we can get to $\langle S_{12} \rangle \approx -0.25$ for $U/\Gamma = 2$. We therefore realize a mixed state with singlet correlations dominating over triplet correlations. The steady-state values further depend on U/Γ . To elucidate this, we plot $\langle S_{12} \rangle$ versus U in the inset of Fig. 3(b) for a fixed value of $V = 0.5$. As expected, the larger U , the more strongly charge fluctuations are suppressed, leading to larger steady-state spin correlations.

So far we have investigated the dependence of correlations on V and ϕ in non-equilibrium, comparing the cases of $\phi = 0$ to $\phi = \pi$. An additional degree of tunability can be added if the phase can take arbitrary values. To illustrate this as-

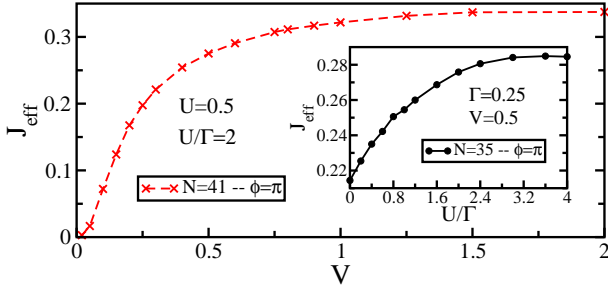


FIG. 4. (Color online) Effective J_{eff} for DQD system as a function of V (main panel) and U (inset) calculated for $\phi = \pi$. Same parameters as in Fig. 3(b).

pect, we display the static spin correlations (i.e., those at $V = 0$) and the steady-state correlations (here for $V = 0.5$) in Fig. 3(c). As expected from the discussion of Fig. 2, $\langle S_{12} \rangle$ is positive for small ϕ at $V = 0$ and then decreases to zero as $\phi = \pi$ is approached. This transition to the uncorrelated case of $\phi = \pi$ is continuous. At a finite voltage, it is possible to go from positive steady-state correlations to negative ones by changing ϕ . For the parameters of Fig. 3(c), the steady-state correlations change sign at $\phi_c \approx 0.18\pi$. This value depends both on U and V . To summarize, the steady-state correlations can be tuned both in sign and magnitude by changing V , ϕ , and U .

Based on the qualitative picture developed so far, we conclude that the steady-state correlations are a result of mixing the symmetric and antisymmetric states of lead electrons in non-equilibrium. At finite U , this may be viewed as an RKKY effect in non-equilibrium. To estimate the strength J_{eff} of the effective coupling between the localized spins in the dots in the steady state, we proceed as follows. First, in the set-up shown in Fig. 2(b.1), we connect the impurities by an additional term $J_{\text{eff}} \vec{S}_1 \cdot \vec{S}_2$ and we then calculate the equilibrium correlations $S_{12} = S_{12}(J_{\text{eff}})$ in this reference system. In the next step, we use the numerically determined function $\langle S_{12} \rangle = \langle S_{12} \rangle(V)$ and by equating it to $S_{12}(J_{\text{eff}})$, we obtain $J_{\text{eff}} = J_{\text{eff}}(V)$, keeping all other parameters fixed in both the time-dependent simulation and in the reference system. The results are presented in Fig. 4 and its inset.

Finally, we study the robustness of the steady-state spin correlations against quenching certain parameters of the Hamiltonian Eq. (1). We proceed as before, i.e., a finite bias voltage $V > 0$ is turned on at $t = 0$, and in addition we perform quenches of either the phase ϕ or some of the tunnel couplings at a time $t_q \geq 0$.

The first example, presented in Fig. 5(a), consists of changing the phase from 0 to π . We show results for $t_q = 0$ and 10 and observe that in both cases, the spin correlations change from their initial constant and positive value to a negative value that only depends on parameters in the steady state (i.e., V and ϕ), but as this comparison shows, is virtually independent of the specific transient dynamics.

In the second case, presented in Fig. 5(b), we simply dis-

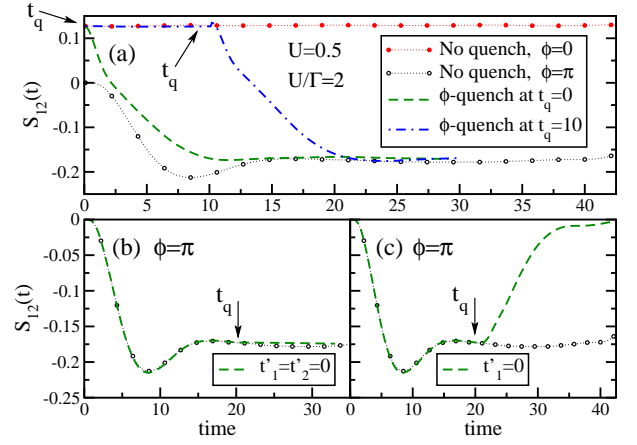


FIG. 5. (Color online) Behavior of the spin correlations in various quantum quenches. (a) Quench of the phase ϕ from $\phi = 0$ to $\phi = \pi$ at a time $t_q = 0, 10$ (dashed and dot-dashed curves). (b) Quench of the hopping matrix elements t'_1 and t'_2 to zero at $t_q = 20$. This decouples the DQD from the leads. (c) Quench of just t'_1 to zero at time $t_q = 20$, effectively decoupling dot 1 while the current continues to flow through dot 2. In all cases, we start with the usual protocol, i.e., we quench the bias from zero to $V = 0.5$ at $t = 0$. For comparison, the data from Fig. 1(b) without any additional quenches are included (lines with open/solid circles are for $\phi = \pi$ and $\phi = 0$, respectively). In all panels, the time t_q at which the quench is performed is indicated by arrows. In this figure, $U/\Gamma = 2$, $V = 0.5$, and $N = 41$.

connect the quantum dots from the leads at time $t_q > 0$ after the steady state has been established. As expected, the spins remain in a correlated state after isolating them from the reservoirs. In order to extract pure singlets from this mixed entangled state [26, 27] one would need to be able to reach spin correlations $\langle S_{12} \rangle < -1/4$ [27, 28], while charge fluctuations render the absolute value of steady-state correlations smaller in our case.

Third, after reaching the steady state, we isolate one of the dots while the current continues to flow through the other one. This results in a destruction of the spin correlations after a short transient time [see Fig. 5(c)]. Therefore, control over the tunneling matrix elements allows one to put the system back into its original uncorrelated state. Both the generation of entanglement and the removal happen on short times scales, similar to the proposals discussed in [13].

Summary: In this work, we demonstrated that spin correlations between spatially separated electrons localized in a parallel DQD embedded in the rings of an Aharonov-Bohm interferometer can be induced and modified by driving a current through the structure. The steady-state correlations depend on voltage, the flux, and Coulomb interactions. Control over the individual tunneling couplings would allow one to isolate the entangled spins from the environment or to remove the entanglement again. The mechanism behind this time-dependent formation of correlations can be thought of as an RKKY effect in non-equilibrium. Our results may be relevant for applications of DQD structures in quantum information processing.

Acknowledgments - We thank S. Andergassen, E.

Dagotto, L.G.G.V. Dias da Silva, A. E. Feiguin, I. Hamad, F. Marquardt, G. B. Martins, G. Roux, and L. Vidmar for helpful discussions. We are indebted to G. Burkard, F. Marquardt, and V. Meden for a critical reading of the manuscript and valuable comments. This work was supported by the *Deutsche Forschungsgemeinschaft* (DFG) through FOR 912 under grant-no. HE5242/2-2.

* carlos.busser@gmail.com

- [1] M. Grobis, I. Rau, R. Potok, and D. Goldhaber-Gordon, “Kondo effect in mesoscopic quantum dot,” (Wiley, 2007); W. G. van der Wiel, S. De Franceschi, J. M. Elzerman, T. Fujisawa, S. Tarucha, and L. P. Kouwenhoven, *Rev. Mod. Phys.* **75**, 1 (2002); R. Hanson, L. P. Kouwenhoven, J. R. Petta, S. Tarucha, and L. M. K. Vandersypen, *ibid.* **79**, 1217 (2007), and references therein.
- [2] A. W. Holleitner, C. R. Decker, H. Qin, K. Eberl, and R. H. Blick, *Phys. Rev. Lett.* **87**, 256802 (2001); W. G. van der Wiel, Y. V. Nazarov, S. D. Franceschi, T. Fujisawa, J. M. Elzerman, E. W. G. M. Huizeling, S. Tarucha, and L. P. Kouwenhoven, *Phys. Rev. B* **67**, 033307 (2003); M. Sigrist, A. Fuhrer, T. Ihn, K. Ensslin, S. E. Ulloa, W. Wegscheider, and M. Bichler, *Phys. Rev. Lett.* **93**, 066802 (2004); J. C. Chen, A. M. Chang, and M. R. Melloch, *ibid.* **92**, 176801 (2004); M. Sigrist, T. Ihn, K. Ensslin, D. Loss, M. Reinwald, and W. Wegscheider, *ibid.* **96**, 036804 (2006).
- [3] Y. Okazaki, S. Sasaki, and K. Muraki, *Phys. Rev. B* **84**, 161305(R) (2011); S. Amasha, A. J. Keller, I. G. Rau, A. Carmi, J. A. Katine, H. Shtrikman, Y. Oreg, and D. Goldhaber-Gordon, *Phys. Rev. Lett.* **110**, 046604 (2013).
- [4] D. Loss and D. P. DiVincenzo, *Phys. Rev. A* **57**, 120 (1998).
- [5] G. Burkard, D. Loss, and D. P. DiVincenzo, *Phys. Rev. B* **59**, 2070 (1999).
- [6] C. H. Bennett and D. P. DiVincenzo, *Nature* **404**, 247 (2000).
- [7] H.-A. Engel, L. Kouwenhoven, D. Loss, and C. Marcus, *Quantum Information Processing* **3**, 115 (2004).
- [8] G. Burkard, D. Loss, and E. V. Sukhorukov, *Phys. Rev. B* **61**, R16303 (2000).
- [9] G. Lesovskii, T. Martin, and G. Blatter, *Eur. Phys. J. B* **24**, 287 (2001); P. Recher and D. Loss, *Phys. Rev. B* **65**, 165327 (2002); C. Bena, S. Vishveshwara, L. Balents, and M. P. A. Fisher, *Phys. Rev. Lett.* **89**, 037901 (2002); P. Recher, E. V. Sukhorukov, and D. Loss, *Phys. Rev. B* **63**, 165314 (2001).
- [10] W. D. Oliver, F. Yamaguchi, and Y. Yamamoto, *Phys. Rev. Lett.* **88**, 037901 (2002); D. S. Saraga and D. Loss, *ibid.* **90**, 166803 (2003); A. T. Costa and S. Bose, *ibid.* **87**, 277901 (2001); F. Ciccarello, G. Palma, M. Zarcone, Y. Omar, and V. Vieira, *J. Phys. A: Math. Theor.* **40**, 7993 (2007).
- [11] M. Blaauuboer and D. P. DiVincenzo, *Phys. Rev. Lett.* **95**, 160402 (2005).
- [12] D. Loss and E. V. Sukhorukov, *Phys. Rev. Lett.* **84**, 1035 (2000).
- [13] S. Legel, J. König, G. Burkard, and G. Schön, *Phys. Rev. B* **76**, 085335 (2007); S. Legel, J. König, and G. Schön, *New J. Phys.* **10**, 045016 (2008).
- [14] J. Eckel, F. Heidrich-Meisner, S. Jakobs, M. Thorwart, M. Pletyukhov, and R. Egger, *New J. Phys.* **12**, 043042 (2010).
- [15] S. Andergassen, V. Meden, H. Schoeller, J. Splettstoesser, and M. R. Wegewijs, *Nanotech.* **21**, 272001 (2010), and references therein.
- [16] W. G. van der Wiel, S. D. Franceschi, T. Fujisawa, J. M. Elzerman, S. Tarucha, and L. P. Kouwenhoven, *Science* **289**, 2105 (2000); M. Grobis, I. G. Rau, R. M. Potok, H. Shtrikman, and D. Goldhaber-Gordon, *Phys. Rev. Lett.* **100**, 246601 (2008); C. Latta, F. Haupt, M. Hanl, A. Weichselbaum, M. Claassen, W. Wuester, P. Fallahi, S. Faelt, L. Glazman, J. von Delft, H. E. Treci, and A. Imamoglu, *Nature* **474**, 627 (2011).
- [17] G. Vidal, *Phys. Rev. Lett.* **93**, 040502 (2004); A. Daley, C. Kollath, U. Schollwöck, and G. Vidal, *J. Stat. Mech.: Theory Exp.* **2004**, P04005; S. R. White and A. E. Feiguin, *Phys. Rev. Lett.* **93**, 076401 (2004).
- [18] Supplementary material: Discussion of asymmetric tunnel couplings and supporting figures.
- [19] W. Hofstetter and H. Schoeller, *Phys. Rev. Lett.* **88**, 016803 (2001); V. Apel, M. Davidovich, E. V. Anda, G. Chiappe, and C. A. Büsner, *Eur. Phys. J. B* **40**, 365 (2004); R. Žitko and J. Bonča, *Phys. Rev. B* **74**, 045312 (2006); *Phys. Rev. B* **74** (2006); R. López, D. Sánchez, M. Lee, M.-S. Choi, P. Simon, and K. Le Hur, *Phys. Rev. B* **71**, 115312 (2005); L. G. G. V. Dias da Silva, N. Sandler, P. Simon, K. Ingersent, and S. Ulloa, *Phys. Rev. Lett.* **102**, 166806 (2009); R. Žitko, J. Mravlje, and K. Haule, *Phys. Rev. Lett.* **108**, 066602 (2012); R. Žitko and J. Bonča, *Phys. Rev. B* **76** (2007).
- [20] D. Boese, W. Hofstetter, and H. Schoeller, *Phys. Rev. B* **64**, 125309 (2001); J. König and Y. Gefen, *ibid.* **65**, 045316 (2002); V. Meden and F. Marquardt, *Phys. Rev. Lett.* **96**, 146801 (2006); V. Kashcheyevs, A. Schiller, A. Aharony, and O. Entin-Wohlman, *Phys. Rev. B* **75**, 115313 (2007); S. Bedkhal and D. Segal, *ibid.* **85**, 155324 (2012).
- [21] K. A. Al-Hassanieh, A. E. Feiguin, J. A. Riera, C. A. Büsner, and E. Dagotto, *Phys. Rev. B* **73**, 195304 (2006); L. G. G. V. Dias da Silva, F. Heidrich-Meisner, A. E. Feiguin, C. A. Büsner, G. B. Martins, E. V. Anda, and E. Dagotto, *Phys. Rev. B* **78**, 195317 (2008); S. Kirino, T. Fujii, J. Zhao, and K. Ueda, *J. Phys. Soc. Jpn.* **77**, 084704 (2008); E. Boulat, H. Saleur, and P. Schmitteckert, *Phys. Rev. Lett.* **101**, 140601 (2008); F. Heidrich-Meisner, G. B. Martins, C. A. Büsner, K. A. Al-Hassanieh, A. E. Feiguin, G. Chiappe, E. V. Anda, and E. Dagotto, *Eur. Phys. J. B* **67**, 527 (2009); F. Heidrich-Meisner, I. González, K. A. Al-Hassanieh, A. E. Feiguin, M. J. Rozenberg, and E. Dagotto, *Phys. Rev. B* **82**, 205110 (2010); A. Branschädel, G. Schneider, and P. Schmitteckert, *Ann. Phys. (Berlin)* **522**, 657 (2010); M. Einhellinger, A. Cojuhovich, and E. Jeckelmann, *Phys. Rev. B* **85**, 235141 (2012); M. Nuss, M. Ganahl, H. G. Evertz, E. Arrigoni, and W. von der Linden, *arXiv:1301.3068*; E. Canovi, A. Moreno, and A. Muramatsu, *arXiv:1301.7683*.
- [22] F. Heidrich-Meisner, A. E. Feiguin, and E. Dagotto, *Phys. Rev. B* **79**, 235336 (2009).
- [23] Finite spin polarizations $\langle \Psi(t) | S_j^z | \Psi(t) \rangle \neq 0$, $j = 1, 2$, on the dots do not occur.
- [24] U. Schollwöck, *Rev. Mod. Phys.* **77**, 259 (2005); *Ann. Phys.* **326**, 96 (2011).
- [25] B. A. Jones and C. M. Varma, *Phys. Rev. B* **58**, 843 (1987); K. Ingersent, B. A. Jones, and J. W. Wilkins, *ibid.* **69**, 2594 (1992); A. E. Feiguin and C. A. Büsner, *Phys. Rev. B* **84**, 115403 (2011); C. A. Büsner and A. E. Feiguin, *ibid.* **86**, 165410 (2012).
- [26] M. Horodecki, P. Horodecki, and R. Horodecki, *Phys. Rev. Lett.* **80**, 5239 (1998).
- [27] N. Linden, S. Massar, and S. Popescu, *Phys. Rev. Lett.* **81**, 3279 (1998).
- [28] R. Werner, *Phys. Rev. A* **40**, 4277 (1989).

Supplementary information for Inducing spin-correlations and entanglement in a double quantum dot through non-equilibrium transport

ASYMMETRIC TUNNEL COUPLINGS

In this supplementary material we show that the key results of our work described in the main text for a DQD with symmetric tunnel couplings carries over to the asymmetric case. We start from the most general form of the Hamiltonian from Eqs. (3) and (4) of the main text. The hybridization between the localized levels of the dots and the leads can be written as

$$H_{\text{hy1}} = -t'_{L1} d_{1\sigma}^\dagger c_{L1\sigma} - t'_{R1} d_{1\sigma}^\dagger c_{R1\sigma} + h.c., \quad (9)$$

$$H_{\text{hy2}} = -t'_{L2} d_{2\sigma}^\dagger c_{L1\sigma} - t'_{R2} e^{i\phi} d_{2\sigma}^\dagger c_{R1\sigma} + h.c., \quad (10)$$

where tunnel matrix elements $t_{\alpha j}$, are considered that can in general be different for each dot ($j = 1, 2$) and lead ($\alpha = L, R$). The tunneling strength is then defined by $\Gamma_j = t_{Lj}^2 + t_{Rj}^2$, $j = 1, 2$. For each dot we introduce an angle θ_j via $\theta_j = \arctan(t'_{Lj}/t'_{Rj})$, and therefore, the terms from Eqs. (9) and (10) can be reexpressed as

$$H_{\text{hyj}} = -\sqrt{\Gamma_j} d_{j\sigma}^\dagger (\sin \theta_j c_{L1\sigma} + \cos \theta_j c_{R1\sigma} + h.c.). \quad (11)$$

We next generalize the canonical transformation of the lead operators that was discussed in the main text in the following way:

$$c_{\mu i\sigma} = (\sin \theta_1 c_{Li\sigma} + \cos \theta_1 c_{Ri\sigma}), \quad (12)$$

$$c_{\nu i\sigma} = (\cos \theta_1 c_{Li\sigma} - \sin \theta_1 c_{Ri\sigma}). \quad (13)$$

In the special case of $\theta_1 = \pi/4$, this reduces to Eq. (8) from the main text with $\mu = s$ and $\nu = a$. Note that the operator $c_{\mu i\sigma}$ defined in Eq. (12) appears directly in H_{hy1} from Eq. (11). Therefore, the QD $j = 1$ is just connected to the μ channel. The resulting configuration, i.e., QD 1 coupled to the μ -channel and QD $j = 2$ coupled to either the μ -, ν -, or both channels is depicted in Fig. 6

The Hamiltonian of the leads H_L with chemical potential $\mu_R = -\mu_L = V/2$ is, under this transformation, given by

$$H_L = H_c + H_V, \quad (14)$$

$$H_c = -t_0 \sum_{\gamma=\mu,\nu} \sum_{i=1}^{N-1} (c_{\gamma i\sigma}^\dagger c_{\gamma i+1\sigma} + h.c.) \quad (15)$$

$$H_V = \sum_{i=1;\sigma}^N [t_p (c_{\nu i\sigma}^\dagger c_{\mu i\sigma} + h.c.) + V_\nu n_{\nu i\sigma} + V_\mu n_{\mu i\sigma}], \quad (16)$$

with

$$t_p = -V \sin \theta_1 \cos \theta_1, \quad (17)$$

$$V_\mu = -V_\nu = \frac{V}{2} (\cos^2 \theta_1 - \sin^2 \theta_1). \quad (18)$$

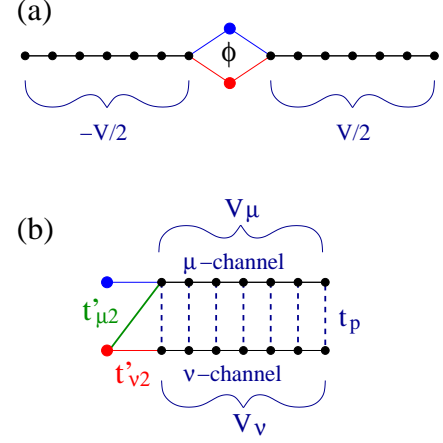


FIG. 6. Sketch of the representation of the DQD structure and its coupling (a) the original leads and (b) the effective leads defined in Eqs. (12) and (13). We refer to the effective leads as the μ - and ν -channel, respectively.

Similar to the case of fully symmetric couplings shown in Fig. 2 of the main text, the bias potential connects the channels μ and ν through an effective coupling t_p . This coupling takes its maximum value in the case of symmetric couplings for QD $j = 1$, i.e., $t'_{L1} = t'_{R1}$ and therefore, $\theta_1 = \pi/4$.

Next, the second QD is connected to the new channels μ and ν through:

$$H_{\text{hy2}} = \sum_{\sigma} (t'_{\mu 2} d_{2\sigma}^\dagger c_{\mu 1\sigma} + t'_{\nu 2} d_{2\sigma}^\dagger c_{\nu 1\sigma} + h.c.) \quad (19)$$

with

$$t'_{\mu 2} = \sqrt{\Gamma_2} (\cos \theta_2 \cos \theta_1 + \sin \theta_2 \sin \theta_1 e^{i\phi}), \quad (20)$$

$$t'_{\nu 2} = \sqrt{\Gamma_2} (-\cos \theta_2 \sin \theta_1 + \sin \theta_2 \cos \theta_1 e^{i\phi}). \quad (21)$$

It is straightforward to verify that $|t'_{\mu 2}|^2 + |t'_{\nu 2}|^2 = \Gamma_2$.

Figure 7 shows, for $\phi = 0, \pi/2$ and π , the square modulus of $t'_{\mu 2}$ and $t'_{\nu 2}$ as a function of θ_1 and θ_2 for $U = 0.5$, $\Gamma_1 = \Gamma_2 = 0.25$, $N = 35$. For $\phi = 0$ and $\phi = \pi$ we observe diagonal stripes where $t'_{\mu 2}$ or $t'_{\nu 2}$ vanish resulting in the situation depicted in Figs. 2 (a) and (b) from the main text. For $\phi = 0$ it is obvious that, if $\theta_2 = \theta_1$, the canonical transformation will decouple both QDs from the ν -channel at the same time as both dots have the same asymmetry.

In order to reproduce the features of Fig. 2 of the main text for the case of asymmetric couplings, we require that either $t'_{\mu 2}$ or $t'_{\nu 2}$ be close to zero. To illustrate this we have selected eight parameter sets for the tunneling matrix elements and the flux ϕ that reproduce such situations, which we list in Table I. Each set of parameters contained in this table is labeled by a letter A, B, ..., G.

Set A is the completely symmetric situation with $\phi = 0$ that we discussed in the main text. In this case, $t'_{\mu 2}/\sqrt{\Gamma_2} = 1$ and $t'_{\nu 2} = 0$. Therefore, QD $j = 1$ and $j = 2$ are connected to the same effective lead and the spin correlations are positive in the

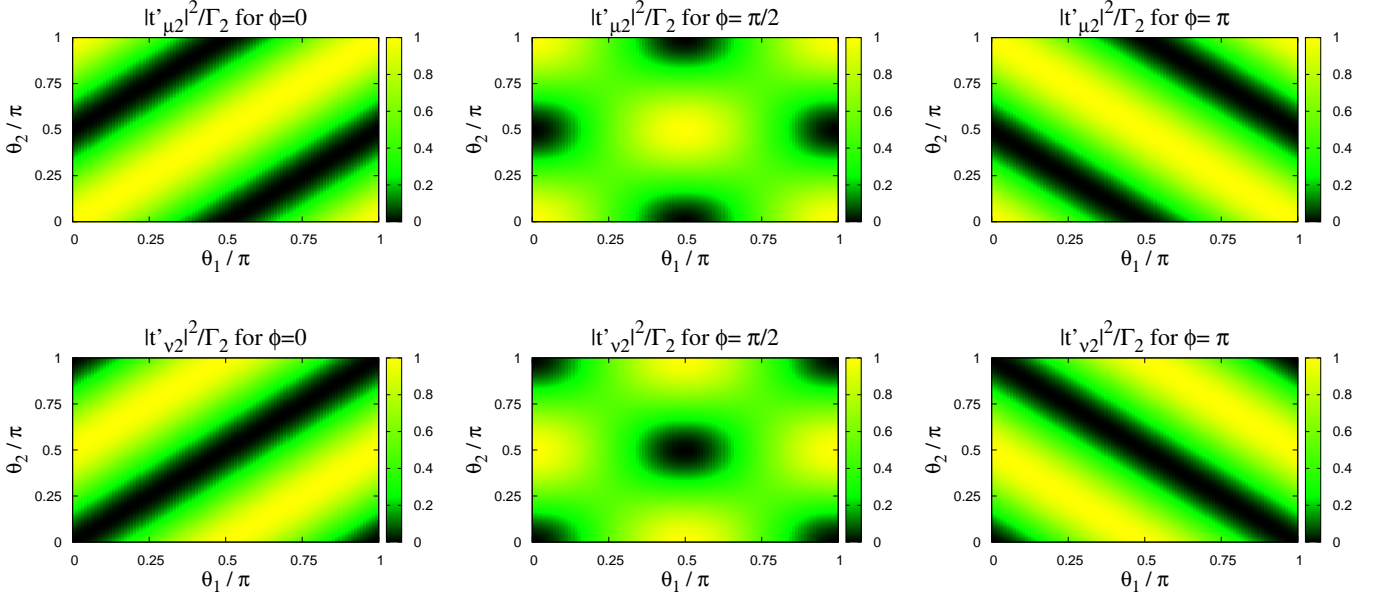


FIG. 7. Square modulus of the couplings between QD $j = 2$ and the effective channels μ and ν defined in Eq. (12) and (13). All curves are for $\Gamma_2 = 0.25$, $U = 0.5$, $V_g = -U/2$ and $N = 35$. To reproduce the features of Figs. 2(a) and (b) of the main text, we need to require $|t'_{\nu 2}|^2 = 0$ or $|t'_{\mu 2}|^2 = 0$, respectively. Note that $t'_{\mu 2}$ and $t'_{\nu 2}$ do not depend on Γ_1 .

Set	θ_1/π	θ_2/π	t'_{l1}	t'_{r1}	t'_{l2}	t'_{r2}	ϕ/π	$ t'_{\mu 2} ^2/\Gamma_2$	$ t'_{\nu 2} ^2/\Gamma_2$	t_p/V	V_μ/V	$\langle S_{12} \rangle$
A	0.25	0.25	0.353	0.353	0.353	0.353	0.0	1.000	0.000	0.500	0.000	> 0
B	0.09	0.89	0.139	0.480	0.169	-0.470	1.0	0.996	0.004	0.267	0.422	> 0
C	0.48	0.47	0.031	0.499	0.497	-0.047	0.2	0.997	0.003	0.067	-0.496	> 0
D	0.25	0.25	0.353	0.353	0.353	0.353	1.0	0.000	1.000	0.500	0.000	< 0
E	0.14	0.64	0.213	0.452	-0.213	0.452	0.0	0.000	1.000	0.385	0.318	< 0
F	0.07	0.43	0.110	0.488	0.488	0.110	0.5	0.090	0.910	0.212	0.452	< 0
G	0.12	0.63	0.184	0.465	0.459	-0.198	0.2	0.049	0.951	0.342	0.364	< 0

TABLE I. Relationship between the bare parameters of the system [see Eqs. (9) and (10)] and the tunnel matrix elements of the effective channels μ and ν [compare Eqs. (11) and (19)]. In this table we show a few examples for which the discussion of the main article applies even for an asymmetric coupling. We choose $\Gamma_1 = \Gamma_2 = 0.25$ for simplicity. In the last column we list the expected sign of the spin correlations.

steady state. A similar behavior is realized for sets B and C. Set B corresponds to a situation in which $\phi = \pi$ while set for C, we choose $\phi = 0.2\pi$. Note that in set B the phase changes the sign of t'_{R2} and the situation is thus similar to set A. In set C, all four couplings, t'_{L1} , t'_{R1} , t'_{L2} , and t'_{R2} , are different from each other and for the selected value of the phase $\phi = 0.2\pi$, no signs are affected.

The examples labeled D to G are cases in which $t'_{\mu 2}$ is small, and therefore, where, according to the picture put forward in the discussion of Fig. 2(b) of the main tex, we expect negative spin correlations in the steady state. Set D is the completely symmetric case with $\theta_1 = \theta_2 = \pi/4$ and $\phi = \pi$. This case was analyzed in the main article and is shown here for comparison. For set E, although $\phi = 0$, there is a difference of $\pi/2$ between θ_1 and θ_2 , resulting in a behavior similar to set D, despite the left-right asymmetry present in set E. Note that t'_{L2} is negative as a consequence, and therefore, the steady-

state spin correlations are also negative, in accordance with the discussion of the main article. The set F realizes a case with $\phi = \pi/2$ and a small $t'_{\nu 2} \sim 0.09$. In this example, left-right symmetry is broken but there are still just two different values for the four tunnel matrix elements $t'_{\alpha j}$. Finally, in set G, $\phi = 0.2\pi$ and all four tunnel matrix elements are different. The very small value of $t'_{\nu 2}$ implies negative steady-state spin correlation as before.

To verify our predictions for the sign of steady-state spin correlations that are based on the numbers listed Table I, we have calculated the spin correlation as a function of time. The results are shown in Fig. 8. Sets A, B and C, as they all have a small value of $t'_{\mu 2}$, lead to a positive spin correlation positive in the initial state ($t = 0$) whose sign and absolute value are barely affected by the bias at all. Sets D, E, F and G all have a small value for $t'_{\nu 2}$. As a consequence, the dots are predominantly connected to one of the two channels μ or ν [compare

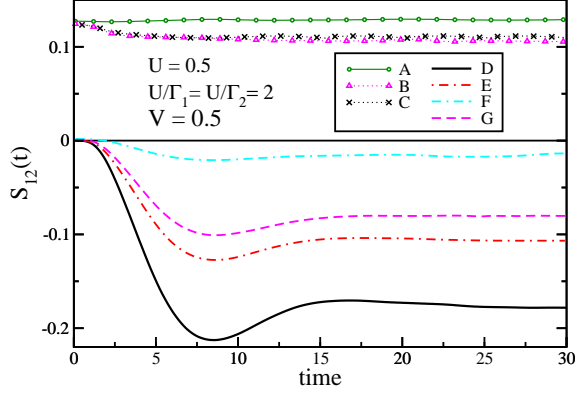


FIG. 8. Spin correlations as a function of time for the parameter sets presented in Table I. Note that for sets with small values of $t'_{\nu 2}$, such as A, B and C, the spin correlations do practically not change when the bias is applied. By contrast, whenever $t'_{\mu 2}$ is small, as is the case in sets D, E, F and G, the spin correlations in the steady state are negative. Sets A and D are the cases discussed in the main text, compare Fig. 1(b).

Fig. 2(b.1) of the main text] and spin correlations vanish in equilibrium, i.e., at for $V = 0$. Upon applying a bias, negative spin correlations emerge, as expected. Note the small value of the steady-state spin correlation in set F, consistent with the observation that in this case, the value of the coupling between the effective leads t_p is the smallest.

As a conclusion, even for asymmetric tunnel couplings between the DQD and the leads the application of a voltage can induce and change spin correlations, which is the main result of our work. The main requirement to obtain a large effect of the bias V on the non-equilibrium spin correlations is a small value of either $t_{\mu 2}$.